

Meridional zonation of the Barents Sea ecosystem inferred from satellite remote sensing and in situ bio-optical observations

B. GREG MITCHELL, ERIC A. BRODY, EUENG-NAN YEH, CHARLES MCCLAIN, JOSEFINO COMISO, and NANCY G. MAYNARD



Mitchell, B. G., Brody, E. A., Yeh, E.-N., McClain, C., Comiso, J. C. & Maynard, N. G. 1991: Meridional zonation of the Barents Sea ecosystem inferred from satellite remote sensing and in situ bio-optical observations. Pp. 147-162 in Sakshaug, E., Hopkins, C. C. E. & Øritsland, N. A. (eds.): Proceedings of the Pro Mare Symposium on Polar Marine Ecology, Trondheim, 12-16 May 1990. *Polar Research 10(1)*.

The Barents Sea is a productive, shallow, high-latitude marine ecosystem with complex hydrographic conditions. Zonal hydrographic bands defined by a coastal current, North Atlantic Water, the Polar Front, and the seasonally variable marginal ice edge zone create a meridional zonation of the ecosystem during the spring-summer transition. The features reveal themselves in satellite imagery and by high-resolution (vertical and horizontal) physical-optical-biological sampling.

Surprisingly, the long-term (7-year) mean of Coastal Zone Color Scanner (CZCS) imagery reveals the Barents Sea as an anomalous "blue-water" regime at high latitudes that are otherwise dominated by satellite-observed surface blooms. A combination of satellite imagery and in situ bio-optical analyses indicate that this pattern is caused by strong stratification in summer with surface nutrient depletion. The onset of stratification of the entire region is linked to the extent of the winter ice edge: cold years with extensive sea ice apparently stratify early due to ice melt; warm years stratify later, perhaps due to weaker thermal stratification of the Atlantic waters (e.g. Skjoldal et al. 1987). The apparent "low chlorophyll" indicated by the CZCS 7-year mean is partly due to sampling error whereby the mean is dominated by images taken later in the summer. In fact, massive blooms of subsurface phytoplankton embedded in the pycnocline persist throughout the summer and maintain substantial rates of primary production. Further, these subsurface blooms that are not observed by satellite are responsible for dramatic gradients in the beam (*c*) and spectral diffuse (*k*) attenuation coefficients. The Barents Sea exemplifies the need to couple satellite observations with spatially and temporally resolved biogeographic ecosystem models in order to estimate the integrated water column primary production, mass flux or spectral light attenuation coefficients.

B. Greg Mitchell and Eric A. Brody, Scripps Institution of Oceanography, La Jolla, California 92093-0218, USA; Eueng-Nan Yeh, Charles McClain and Josefino C. Comiso, NASA Goddard Space Flight Center Code 971 Greenbelt, Maryland 20771, USA; Nancy G. Maynard, Office of Science and Technology Policy, Washington, D.C. 20506, USA.*

Introduction

The Barents Sea is a productive high-latitude marine ecosystem dominated by a shallow shelf and complex hydrography (Loeng 1991 and references therein). The region has supported a commercially significant fishery of capelin and cod (Loeng 1989a). An effort to characterize more completely the ecological system was fostered by the Norwegian Research Program for Marine Arctic Ecology (Pro Mare) (Loeng 1989a).

A consistent pattern associated with the hydrography of the Barents Sea is a zonal struc-

turing with the Norwegian Coastal Current flowing northward to the Barents Sea and then eastward in the vicinity of Nordkapp, eventually entering the Kara Sea (Fig. 1). Farther north, a broad band of the Norwegian Current flows out of the Norwegian Sea eastward into the Barents Sea; the location and flow rates are closely coupled to bathymetry, tidal cycles and poorly understood interannual differences in Atlantic Water flow (Ådlandsvik & Loeng 1991 this volume; Støle-Hansen & Slagstad 1991 this volume; Loeng, 1991 this volume). Recirculation of this water to the Norwegian Sea by the Bjørnøya Current and mixing with Arctic Ocean water occurs farther north, near Bjørnøya. The marginal ice zone (MIZ), and its seasonal procession

* Present address: NASA Headquarters Code SEP, Washington, D.C. 20546, USA.

and recession dominate the northern-most region of the Barents Sea. Although this is a highly simplified concept of the regional hydrography, and much topographic, meteorological and tidal forcing is superimposed on the simple scheme, these features nevertheless are manifest as persistent patterns through time (Loeng 1991).

The ecology of the system is strongly influenced by the hydrographic processes (Rey & Loeng 1985; Skjoldal et al. 1987; Rey et al. 1986). The timing and location of the spring bloom and its disappearance are coupled to upper water column stratification, which in turn is dependent on meteorological conditions, particularly temperature, insolation and winds (Rey & Loeng 1985).

In this paper, Coastal Zone Color Scanner (CZCS) imagery for 1979 and 1980 is analyzed with respect to the meridional zonation of the Barents Sea. The data are interpreted with respect to sea ice observations for the same years determined by the Scanning Multichannel Microwave Radiometer (SMMR) sensor, also flown on the Nimbus-7 satellite. Meridional zonation noted in the CZCS imagery is also evaluated with respect to detailed bio-optical-physical profiles and sections measured along 31°30'E during Pro Mare cruise 11 in May and June 1987.

Methods

In situ observations

The optical-physical package consisted of a Biospherical Instruments reflectance spectroradiometer (MER 1012-F), in situ fluorometer (Sea Tech, Inc.), 25 cm transmissiometer centered at 660 nm (Sea Tech, Inc.) and temperature and conductivity probes (Sea Bird Electronics). The system has also been described elsewhere (Mitchell Holm-Hansen 1991a; Mitchell 1991). Eighteen channels were multiplexed and digitized by the MER unit and communicated to the surface as a frequency signal via a standard single conductor oceanographic cable. The optical measurements included profiles of seven channels of downwelling spectral irradiance ($E_d(\lambda)$), 5 channels of upwelling spectral radiance ($L_u(\lambda)$), photosynthetically available scalar irradiance ($E_o(\text{PAR})$ 2- π , 400–700 nm), beam attenuation, flash induced chlorophyll *a* fluorescence, and solar-induced chlorophyll *a* fluorescence (Table 1). Sampling rates were set so that approximately 5 samples

Table 1. Data products from the Bio-optical-physical profiler

$^1E_d(\lambda)$	410, 441, 488, 520, 560, 630, 683
$^2K_{E_d}(\lambda)$	410, 441, 488, 520, 560, 630, 683
$^3L_u(\lambda)$	441, 488, 520, 560, 683
$^4R_{rs}(\lambda)$	441, 488, 520, 560, 683
5E_o	Photosynthetically Available Radiation
Beam attenuation (c)	660 nm
Fluorescence at 685 nm	(Flash and Solar Induced)
Conductivity, Temperature	

¹ Downwelling spectral irradiance

² Diffuse attenuation coefficient for $E_d(\lambda)$

³ Upwelling spectral radiance

⁴ Remote sensing reflectance ratio ($L_u(\lambda)/E_d(\lambda)$)

⁵ Scalar Irradiance for Photosynthetically Available Radiation (PAR)

per meter were acquired while profiling at 20 to 30 m minute^{-1} from 0 to 200 m. The data density in the vertical domain is thus comparable to traditional CTD data. All data from these 18 channels were automatically recorded in our shipboard computer; selected variables were displayed in real time on a video screen. The computer also recorded incident scalar irradiance for photosynthetically available radiation (PAR 400–700 nm) with a 2- π deck cell which was located in a shade-free area of the ship's superstructure. The data and data products derived from the system are presented in Table 1.

Data from the 25 cm transmissiometer were transformed to the beam attenuation coefficient ($c_t \text{ m}^{-1}$; Bartz et al. 1978). Vertical profiles of spectral irradiance at 488 nm were transformed to optical depth (kz) according to:

$$kz(488) = -\ln [E_d(488,z)/E_d(488,0)] \quad (1)$$

where z represents depth and 488 denotes the instrument's spectral band at 488 nm.

Discrete water samples

Chlorophyll concentrations were determined on extracts of samples concentrated by filtration on Whatman GF/F glass fiber filters and extracted in 90% acetone. The fluorometric method of Holm-Hansen et al. (1965) was used for the determinations. The fluorometer was calibrated spectrophotometrically using pure chlorophyll *a* (Sigma Chemical, Inc). Nitrate concentrations were determined with an autoanalyzer using standard colorimetric methods described in Strickland and Parsons (1972). Details of these

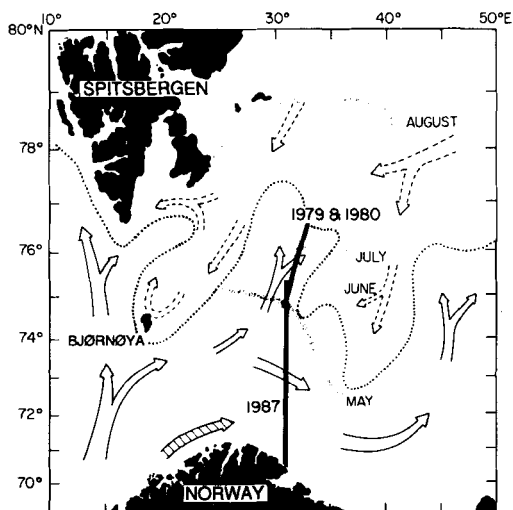


Fig. 1. Map of the Barents Sea study region, with simplified current flow indicated. Solid arrows are flow of Norwegian Sea Water; dashed arrows are flow of Arctic Basin Water and striped arrow is Norwegian Current water. The dotted line represents the typical position of the Polar Front. The typical ice extent in the central Barents Sea each month from May to August is indicated by the shaded lines. Transects that are discussed in the text are indicated by solid lines for 1979, 1980 and 1987.

methods can be found elsewhere (Skjoldal et al. 1987).

Satellite observations

All analysis of satellite imagery was done using the SEAPAK software system (McClain et al. 1991) on the Ocean Computer Facility (OCF) at the Goddard Space Flight Center (GSFC). Imagery from the Coastal Zone Color Scanner (CZCS), operational on the Nimbus-7 satellite from 1978 through 1986, was used to estimate surface distributions of phytoplankton pigments (Gordon et al. 1980; Gordon et al. 1983). The seven year mean data were provided by the GSFC global ocean color project (Feldman et al. 1989).

For the 7-year global CZCS mean pigment data product, high resolution imagery (0.825 km pixel size at nadir) was subsampled to 4 km resolution and processed to produce pigment concentration (chlorophyll *a* + phaeopigment; Gordon et al. 1983). These data were then binned to a 1024 × 2048 element global grid (approximate resolution = 20 km at the equator) and averaged to form the 7-year mean field.

Individual high resolution images were also subsampled and processed to correct for clouds and atmospheric path radiance using the same atmospheric correction and bio-optical algorithm as were used in the global CZCS processing. The pigment scenes were remapped to a common projection. The subsampling was required in order to display and process the data in a 512 × 512 pixel SEAPAK image format. To obtain a largely cloud free image for 1980, three images from consecutive days were averaged after coregistration.

The sea ice distributions were determined using brightness temperature data from the Scanning Multichannel Microwave Radiometer (SMMR), also on-board Nimbus-7. Daily ice concentrations over polar regions were derived from SMMR brightness temperature data using an algorithm described in Comiso (1986). Monthly mean maps were used for the analyses presented here.

Results and discussion

Meridional section along 31°30' E

Although light is acknowledged as a dominant controlling factor for phytoplankton growth, little work has been conducted in Arctic waters using modern in situ optical instrumentation (Mitchell 1991). Such instrumentation was used successfully by us during Pro Mare cruise 11 in May–June 1987. Our bio-optical studies demonstrated the dynamic response of the planktonic community to specific physical–chemical forcing. From 8–10 June 1987 a rapid section along 31°30' E was carried out between the MIZ and Vardø, Norway (Fig. 1). Along this meridional section, distinct hydrographic, and bio-optical zonation was noted. For example, the plankton ecosystem varied depending on whether the hydrography was coastal water (Zone 1), typical Atlantic Water (Zone 2), the frontal mixing zone at the southern boundary of the meltwater where weak stratification induced a phytoplankton bloom (Zone 3), or the MIZ where postbloom sedimentation resulted in a low-nutrient, low-biomass mixed layer with a prominent subsurface pigment maximum (Zone 4).

Fig. 2 illustrates the vertical structure of the biological, optical, and physical properties of the water column for these zones; Fig. 3 illustrates the section encompassing all zones for σ_t , nitrate

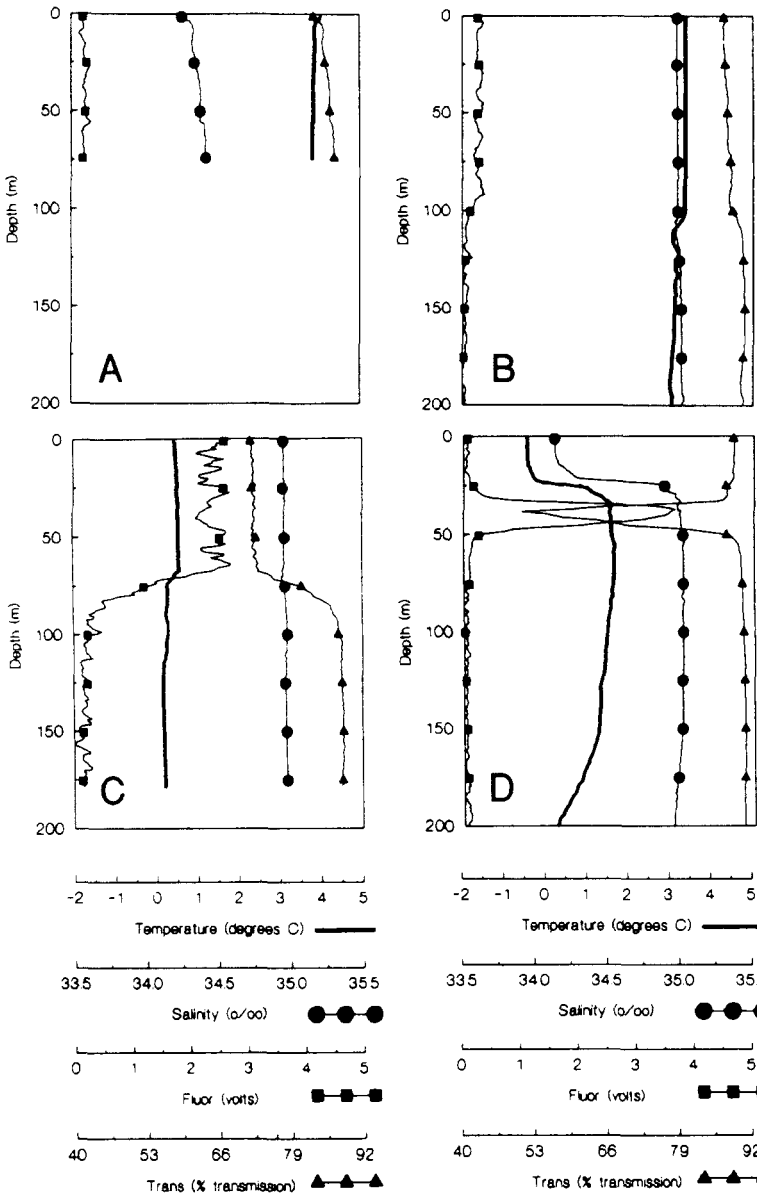


Fig. 2. Vertical profiles of hydrographic and bio-optical properties for different zones of the Barents Sea observed on a transect along 31°30' E from 8–10 June, 1987. In these figures, the values for percentage transmission are for a 25 cm path. A. Zone 1 coastal water. B. Zone 2 deeply mixed, pre-bloom Atlantic Water. C. Zone 3 weakly stratified water with maximum bloom conditions. D. Zone 4 stratified Arctic Water at the MIZ with dramatic subsurface maxima in particles and chlorophyll *a* (minimum in transmission). Symbols on curves are for reference to the legends; actual sampling was nominally at 5 m⁻¹ averaged to 1 m intervals.

and chlorophyll *a*, and Fig. 4 is the section for c_t and $k_z(488)$. Zone 1 was south of 71°N; Zone 2 was in the vicinity of 72°N; Zone 3 was in the vicinity of 74°30'N; and Zone 4 was at the MIZ near 75°30'. In the Coastal Current (Zone 1, Fig. 2A) the water column was weakly stratified and nutrients (Fig. 3B) were relatively low as were chlorophyll *a* concentrations (Fig. 3C), resulting in small values of c_t (Fig. 4A). These observations suggest the coastal region had bloomed earlier,

depleting the nutrients. Apparently, sufficient time had passed for the bloom to be reduced by grazing or sedimentation. In Zone 2 (Fig. 2B) we observed a prebloom situation in Atlantic waters. Density stratification was minimal. Phytoplankton biomass was low ($< 0.5 \text{ mg chlorophyll } a \text{ m}^{-3}$) as indicated by low in situ fluorescence and low beam attenuation coefficients. The low diffuse attenuation coefficient resulted in a 50 m depth of the 1% level for 488 nm light (Fig. 4B). Farther

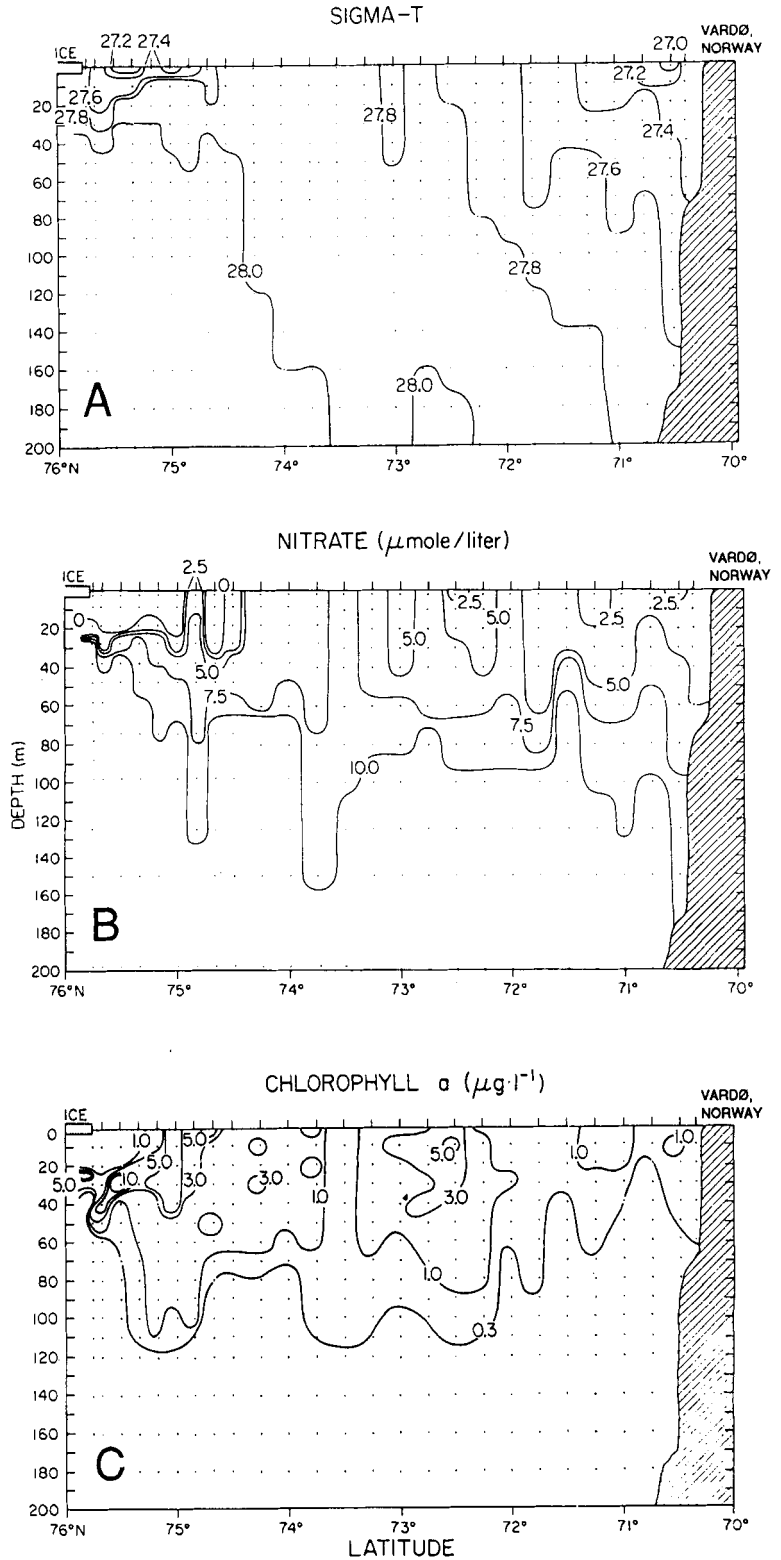


Fig. 3. Sections along 31°30'E. during the period 8–10 June, 1987. See Fig. 1 for location of transects. A. Density. B. Nitrate. C. Chlorophyll a . For comparison to Fig. 2, Zone 1 was south of 71°N; Zone 2 was in the vicinity of 72°N; Zone 3 was in the vicinity of 74°30'N; and Zone 4 was at the MIZ north of 75°30'N.

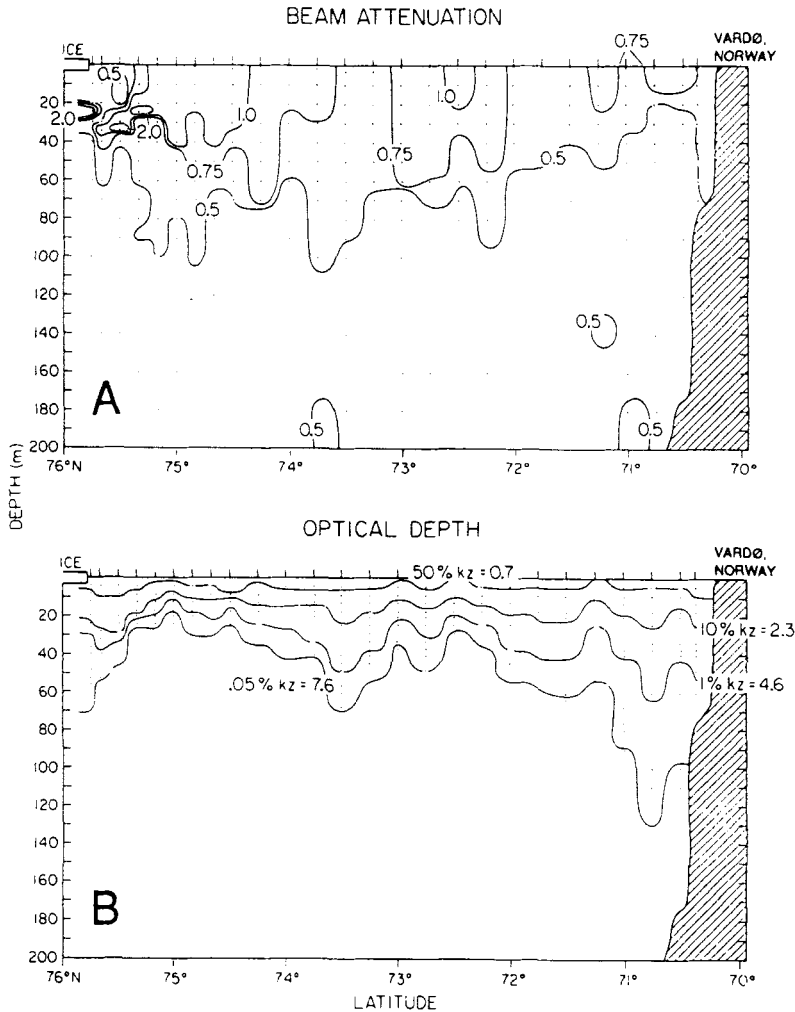


Fig. 4. Sections along $31^{\circ}30'E$. during the period 8–10 June, 1987. A. Beam attenuation coefficient (c_t). B. Optical depth, k_z for 488 nm light. The percentages of 488 nm surface irradiance corresponding to each $k_z(488)$ isolume are also provided.

north (Zone 3, Fig. 2C) the water column was characterized by a slight stratification at approximately 40 m. This was sufficient to promote phytoplankton growth and sustain high biomass ($>5.0 \text{ mg chlorophyll } a \text{ m}^{-3}$) as a response to higher irradiance in the shallower mixed layer. Beam attenuation (c_t) and fluorescence were high while the 1% light level for 488 nm was at 20 m. At the ice edge (Zone 4, Fig. 2D), a postbloom condition was evident since biomass and nutrients were low in a shallow mixed layer (20 m) above a strong pycnocline at 25 m (Fig. 3). The phytoplankton were present in a sharp subsurface ($>5.0 \text{ mg chlorophyll } a \text{ m}^{-3}$) maximum at 25 m corresponding to maxima in the beam attenuation coefficient (c_t) and strong gradients in the diffuse attenuation coefficient (k) (Fig. 4).

Satellite-derived surface pigment distributions

Consistent with the meridional zonation of in situ properties, the 7-year global mean pigment concentrations from the CZCS also exhibits a north-south zonation (Fig. 5). Blooms are noted in the coastal current, the north Atlantic waters, and the Greenland Sea; the northern Barents Sea, near the MIZ, appears to have pigment concentrations of approximately $0.3 \text{ mg (chl + phaeo) m}^{-3}$. Such low values are comparable to the transition zones of the subarctic gyres or the western Mediterranean Sea.

When evaluating imagery such as this, one must bear in mind that the CZCS signal is derived predominantly from less than one optical depth, which is typically less than 20 m (Gordon &

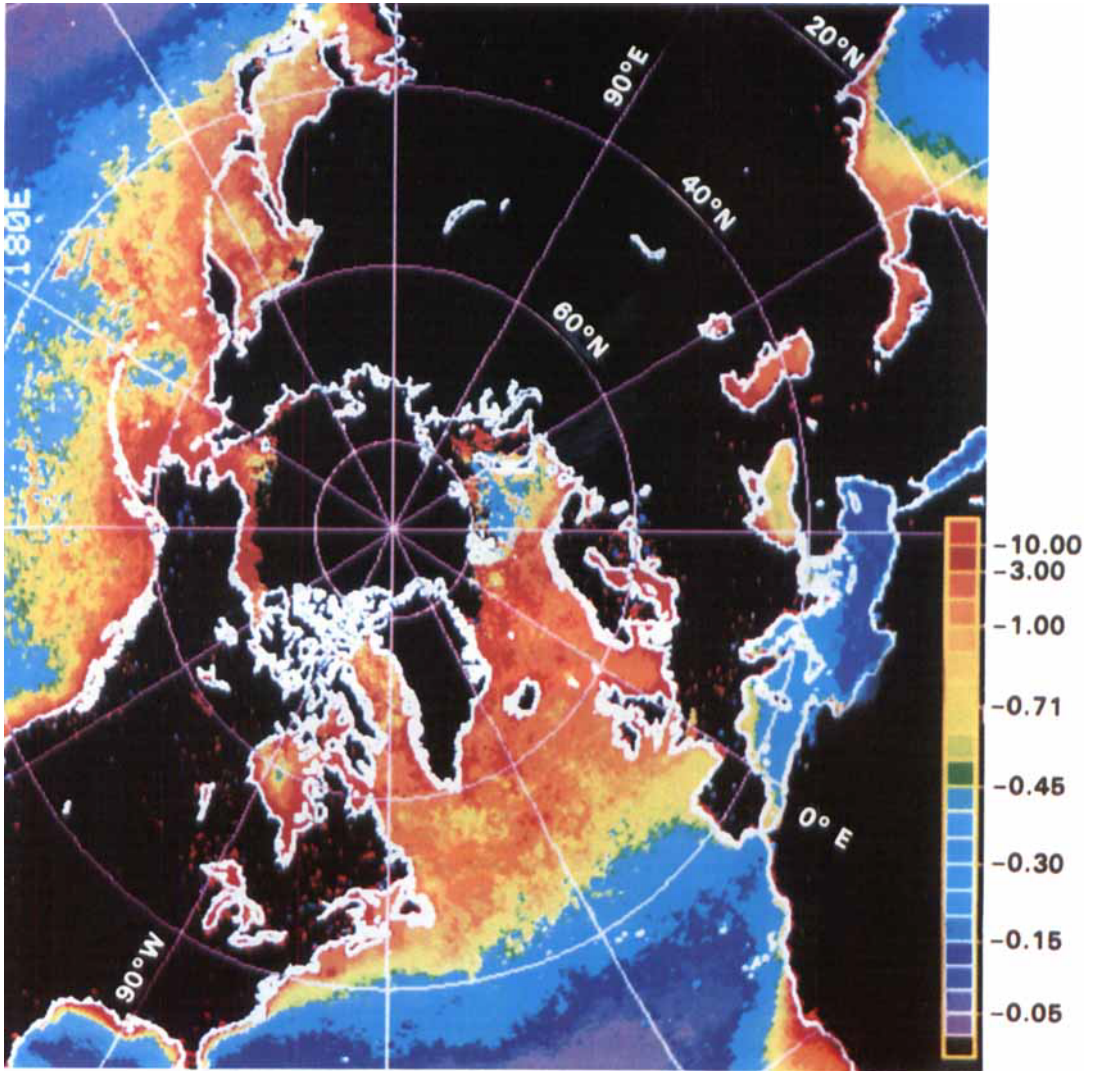


Fig. 5. North polar view of the 7-year global mean of CZCS data. The color scale ranges from violet ($0.05 \text{ mg (chl + phaeo) m}^{-3}$) to red ($10 \text{ mg (chl + phaeo) m}^{-3}$). Note the meridional zonation of the Barents Sea. The northern Barents Sea appears to be an "oligotrophic" body of water. Temporal sampling bias, and an inability of ocean color imagers to resolve massive subsurface blooms in the Barents Sea contribute to this misperception.

McCluney, 1975). Further, the 7-year mean is not a random sampling of the data and is especially biased temporally for high latitudes. An evaluation of the sampling statistics for a $600 \times 600 \text{ km}$ box centered at 31°E and 75°N revealed that no observations were collected for the 7-year mean product in autumn or winter.

The actual mean estimates were calculated, on the average, from 2.4 observations per pixel in spring and 4.1 observations per pixel in summer.

The seasonal means for the 7 year CZCS data set are shown in Fig. 6(a) and b) for spring and summer, respectively. Spring conditions indicate substantial surface blooms, up to 10 mg

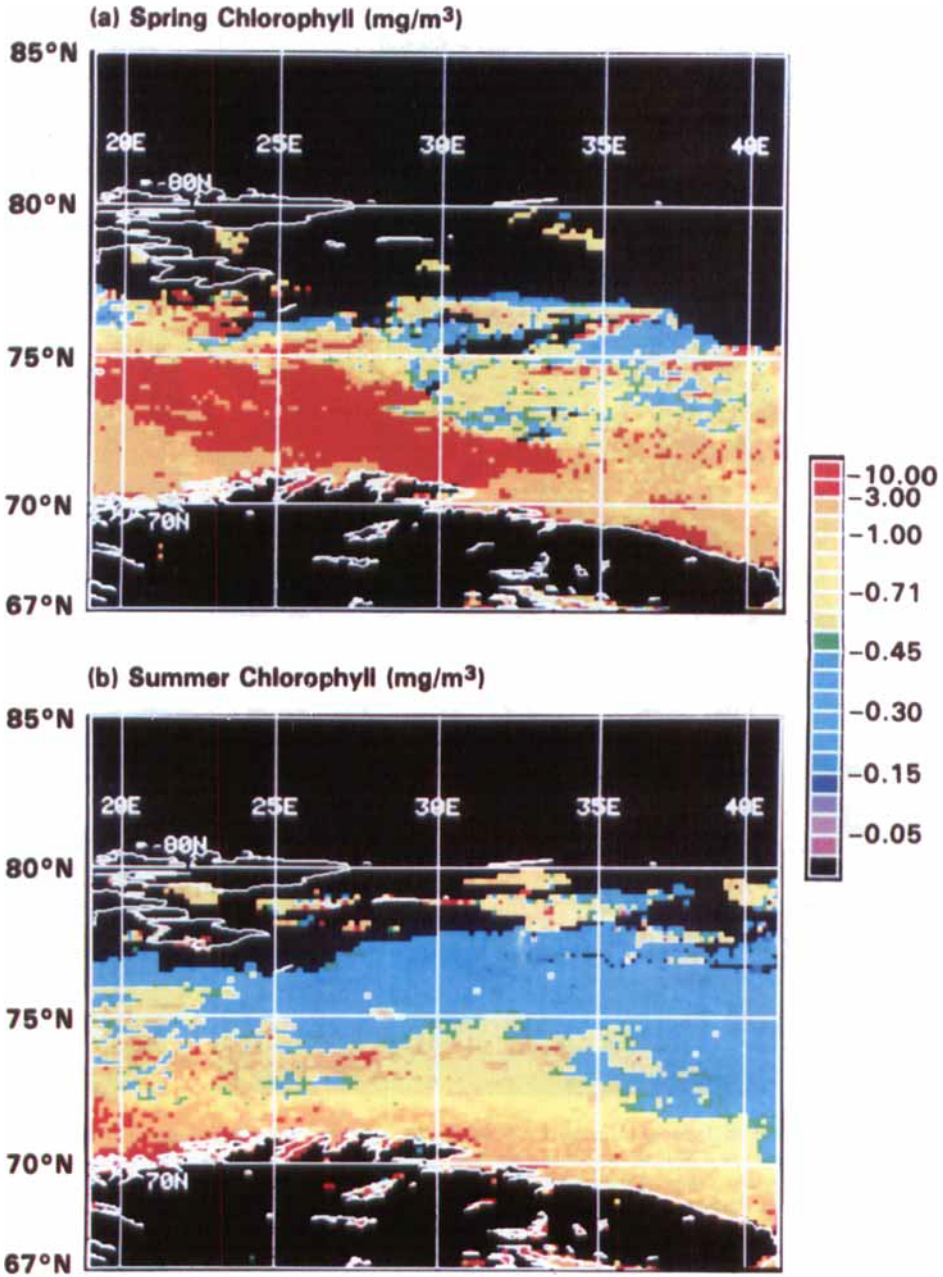


Fig. 6. The spring and summer seasonal mean CZCS from the 7-year CZCS data set. Meridional zonation is more pronounced in summer. In the vicinity of 31°E and 75°N each pixel represents, on the average, 2.4 observations in spring and 4.1 observations in summer.

chl + phaeo m^3 . During the summer, the surface blooms are substantially reduced and are restricted to the coastal and Atlantic waters; Arctic waters farther north exhibit very low surface phytoplankton concentrations. Apparently high values at the ice edge may be artifacts of "ringing", which is the result of amplifier oscillation that occurs when the scan passes from a very bright target (i.e. ice and clouds) to relatively dark targets as it scans a swath across the orbital track (Mueller 1988). Values observed in the MIZ may not be accurate: low pigment values along the eastern (downscan) edge of clouds may be artifacts of "ringing". Also, some high values observed in the MIZ may be artifacts of suspended ice crystals and subpixel-sized ice segments which perturb the observed radiance but not to the level that triggers the cloud/ice flag.

Both spring and summer seasons exhibit the characteristic zonal structuring although it is much more pronounced in summer. Clearly, given the temporal sampling bias of the long-term mean, and the very few actual samples observed during seven years for each pixel, a significant statistical sampling error can lead to erroneous conclusions regarding instantaneous processes at less than seasonal time scales. In this case, the dominance of summer observations biases the seven year mean toward a summer type scenario (Zone 4, Fig. 2D).

CZCS images in early summer 1979 and 1980 and ship-based validation

The CZCS was considered an experimental "proof-of-concept" satellite mission. Due to limited power and data storage capability aboard Nimbus-7, the CZCS instrument had a duty cycle of only about 10%; most of the coverage was for temperate-zone oceans. Combined with the predominantly cloudy conditions of high-latitudes, relatively little useful imagery is available for the Barents Sea. However, good interannual comparison is possible for early July 1979 and late June 1980. The 10 July 1979 image indicates quite low pigment concentrations throughout the Barents, Norwegian and Greenland Seas (Fig. 7(a)). Concentrations of $<0.4 \text{ mg (chl + phaeo) m}^{-3}$ dominate the Barents Sea while a bloom of $>1 \text{ mg (chl + phaeo) m}^{-3}$ is noted in the Norwegian Sea. Clouds obscure most of the region of Atlantic waters north of Nordkapp, but on the eastern

edge of the clouds a bloom of approximately $1 \text{ mg (chl + phaeo) m}^{-3}$ is present.

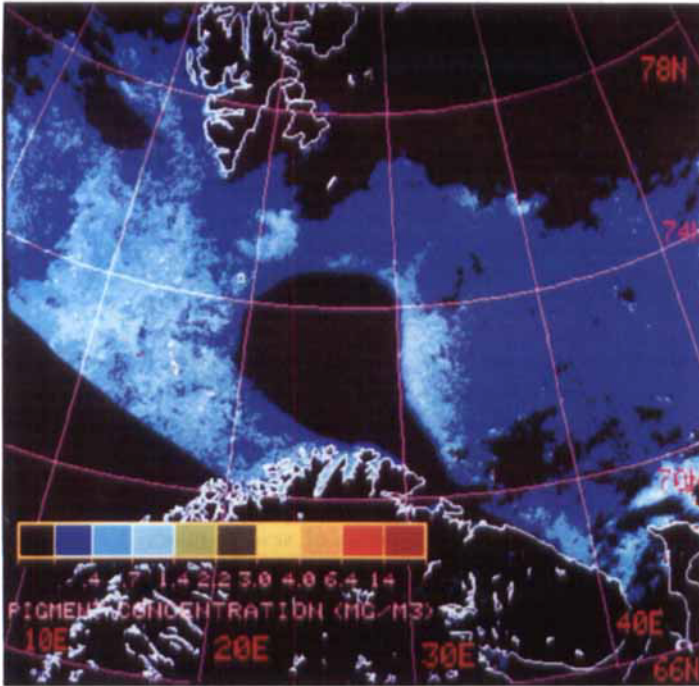
By contrast, the composite image for 28–30 June 1980 indicates an extensive bloom with pigment concentrations of 3–10 mg (chl + phaeo) m^{-3} in the western Norwegian and Greenland Seas, with a comparable bloom in the Norwegian Sea and coastal waters of the Barents Sea (Fig. 7(b)). Only the northern and eastern-most regions of the Barents Sea, near the ice edge, exhibit low pigment concentrations. Interannual variations in primary production, fish yield and plankton (both phyto- and zooplankton) have been well documented using ship observations (Skjoldal et al. 1987; Loeng 1989a; Loeng 1989b). The images in Fig. 7 are a demonstration that the differences in phytoplankton concentrations can be observed using future satellite ocean color imagery, promising the hope of real-time synoptic information for fisheries policy decisions.

An evaluation of several hundred scenes of CZCS imagery for the Barents Sea during the entire seven-year cycle resulted in very few images with sufficiently cloud free conditions to illustrate the typical zonation and structure of the Barents Sea. The best imagery is represented by the data in Fig. 7. Fortuitously, Skjoldal et al. (1987) carried out north-south sections near 31°E with precise coincidence to the CZCS observations shown in Fig. 7. Their data for nitrate and chlorophyll *a* are presented in Fig. 8A and B for 11–12 July 1979 and in Fig. 8C and D for 29–30 June 1980, respectively. Their observations corroborate our two satellite composites in Fig. 7. Minimum and maximum in situ observations for chlorophyll *a* are consistent with the CZCS observations. Surface concentrations observed in situ ranged from 0.02–0.5 mg chlorophyll *a* m^3 in 1979 while they ranged from 0.1–5.0 mg chlorophyll *a* m^3 in 1980. It is evident that in July 1979 the situation was a post-bloom scenario typical of the dominant summer conditions in the Barents Sea: nitrate was depleted in surface waters (Fig. 8A) and a significant sub-surface maximum in chlorophyll *a* was evident (Fig. 8B). The situation in late June 1980 was of a peak bloom induced by thermal stratification in Atlantic Water (Skjoldal et al. 1987) (Fig. 8D).

Comparison of sea ice in 1979 and 1980

To study how the CZCS pigment observations were affected by seasonal and interannual vari-

(a) July 10, 1979



(b) June 28–30, 1980

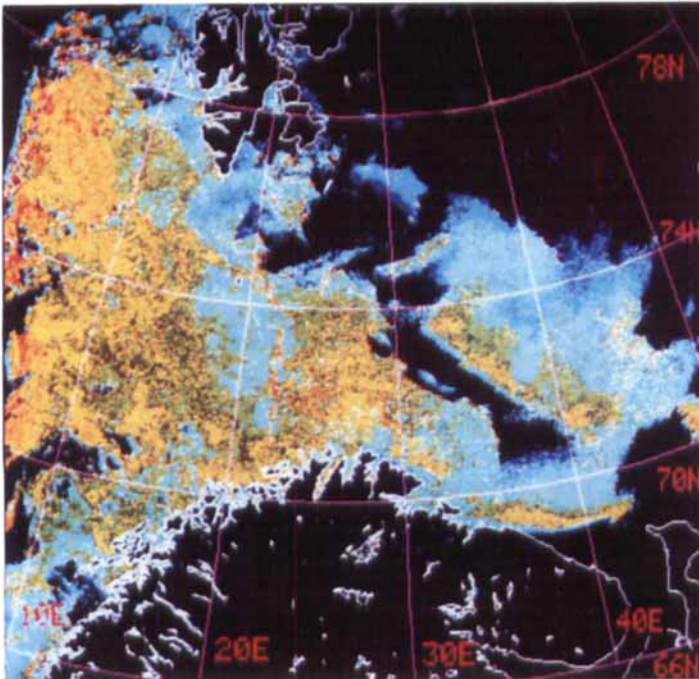


Fig. 7. CZCS imagery of the Barents, Norwegian and Greenland Seas 10 July, 1979 (a) and 28–30 June, 1980 (b). Although the image is for early summer each year, significant interannual variability is evident. The CZCS data agree well with concurrent ship-based observations of Skjoldal et al. (1987). A land mask is indicated by the white borders; a cloud/ice algorithm generated a mask resulting in extensive regions that are obscured in the imagery.

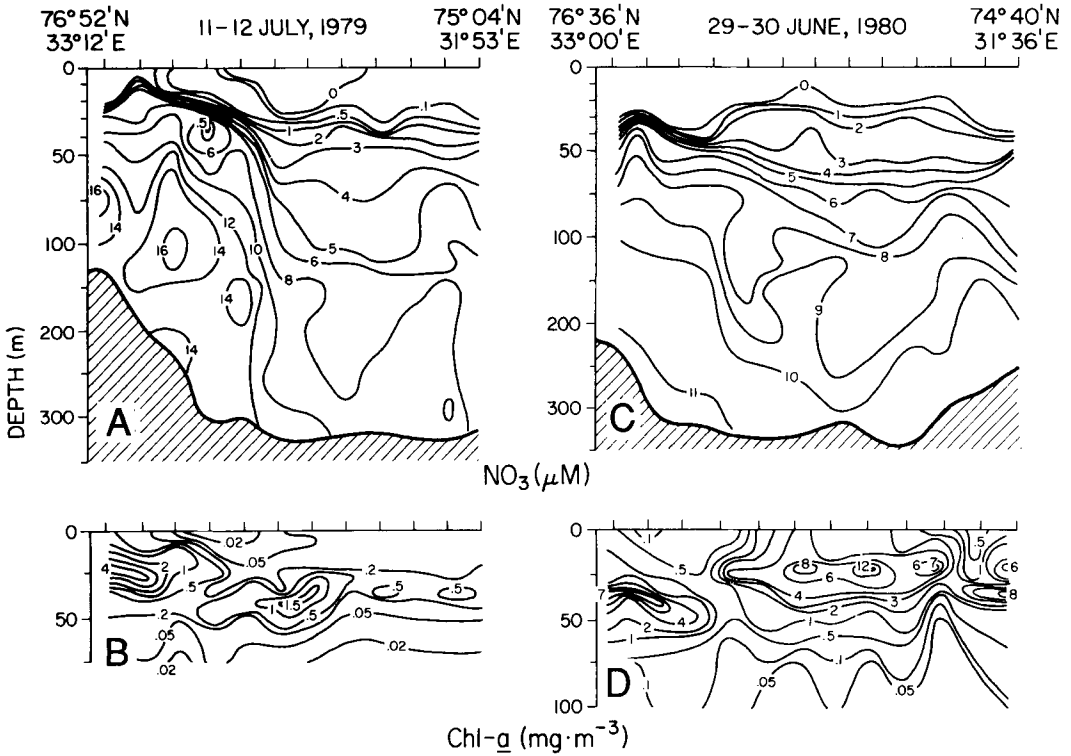


Fig. 8. Ship-based observations from Skjoldal et al. (1987) of nitrate and chlorophyll *a* for 11–12 July 1979 and 29–30 June 1980 along a transect centered about 75°N and 31°E in the central Barents Sea. See Fig. 1 for position of transects. A. Nitrate in 1979. B. Chlorophyll *a* in 1979. C. Nitrate in 1980. D. Chlorophyll *a* in 1980. 1979 was year with heavy ice cover and the Barents Sea was in a post-bloom condition in early summer. 1980 was a year with little ice and the Barents Sea was at peak bloom in early summer.

ations in ice cover, ice maps from the SMMR were analyzed. Monthly averages for February and June of 1979 and 1980 were generated from the daily averages and are shown in Fig. 9. February is generally the month of maximum ice development; June is considered the month most relevant to the conditions at the time of the CZCS observations for the present study. Ice concentrations as high as 108% are in the images because of large variations in the emissivity of sea ice during the spring and summer time period (Comiso 1986). These obvious overestimates due to high emissivities in some regions may be compensated by underestimates due to low emissivities in other regions. It is beyond the scope of the present paper to discuss the error associated with estimates of percentage ice cover; a detailed discussion can be found in Comiso (1986).

The extent of ice is much more accurately determined because of the high contrast of ice and water in the ice margin. In the Barents Sea region,

sea ice is shown to be more extensive in 1979 than 1980, especially the region west of Novaja Zemlja. This is true for February and June. The Greenland Sea region shows a similar pattern. In February 1979 (Fig. 9(a)), the region near 75°N and 45°E shows highly consolidated ice with some low concentration areas near the marginal ice zone indicating new ice production. In contrast to this, an embayment was formed during the early part of the 1980 winter and was never frozen during the rest of the winter (Fig. 9(c)). Further, the February 1980 ice concentrations north of Novaja Zemlja were as low as 70% whereas that region was 100% ice-covered in 1979. The difference image in the ice cover during the two winters is shown in Figure 10(a); areas covered by ice in 1979 but not covered by ice in 1980 are indicated in the image as blue. The difference in ice-covered area in a region bounded by a rectangle defined by 79.5°N, 63.9°E and 68.9°N, 23.3°E was estimated at about 200,000 km².

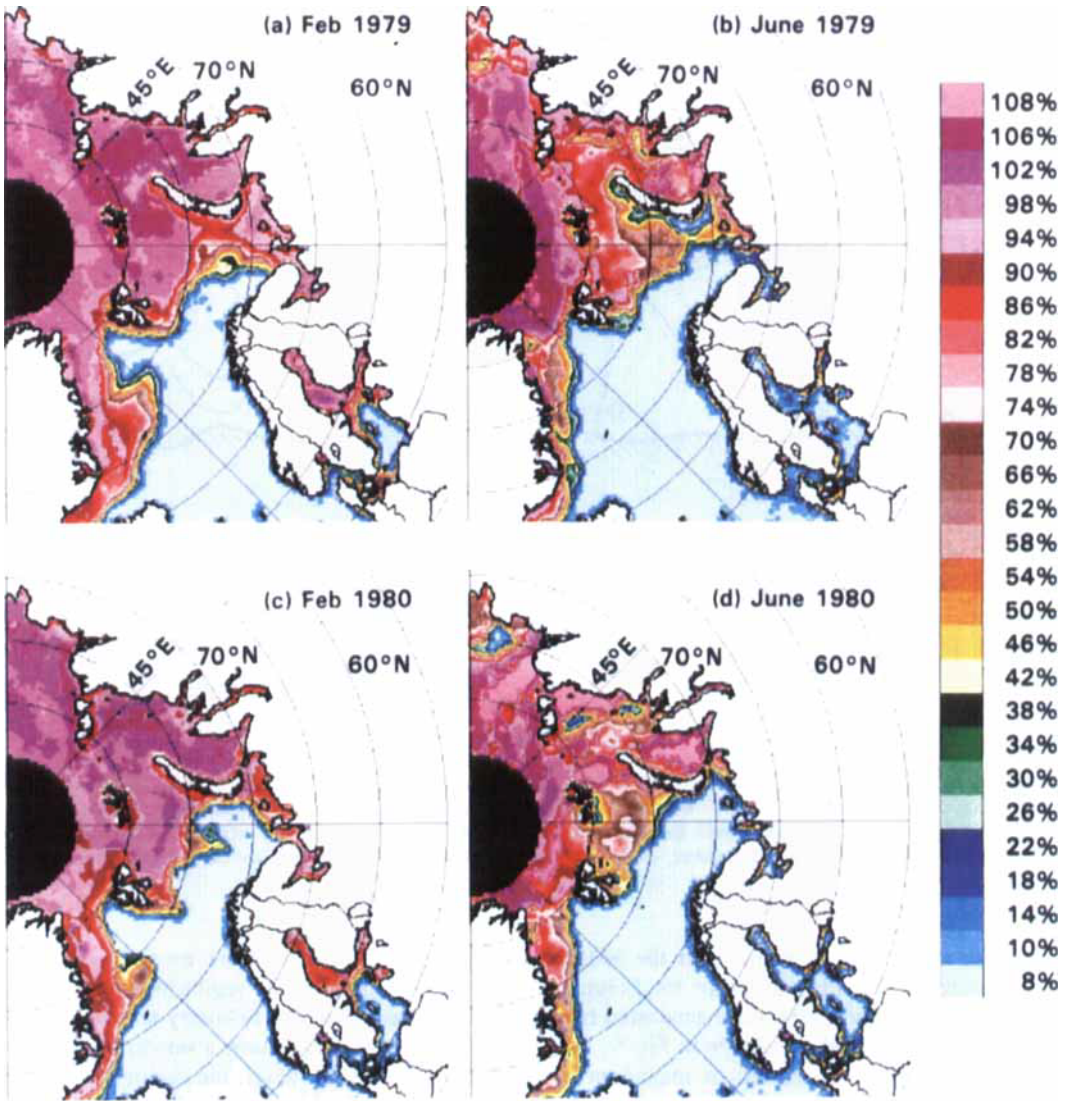


Fig. 9. Seasonal sea ice images derived from the SMMR instrument on NIMBUS-7 for the eastern Arctic: (a) February 1979, (b) June 1979, (c) February 1980, (d) June 1980.

Assuming 1.5 m as the average thickness of ice in the region, the difference in ice volume of resident ice cover during these two periods would be about 300 million m^3 . Thus a substantially greater volume of fresh water from melting ice was available for inducing stability in 1979 compared to 1980.

The June images show a significantly reduced ice cover from the winter time period but not in the same areas for both years. This is better illustrated in the seasonal difference images between February and June of 1979 and 1980 as

shown in Fig. 10(b) and (c), respectively. For 1979, the area of largest retreat is in the east near Novaja Semlja while in 1980, the retreat is more evenly distributed between Novaja Semlja and Svalbard. The seasonal decreases in ice cover from February to June for 1979 and 1980 are 278,000 km^2 and 264,000 km^2 , respectively. The volume of ice melted during the period can be calculated as above, but in addition, there is also some thinning of the ice which survived in June. It is important to note, however, that the volume

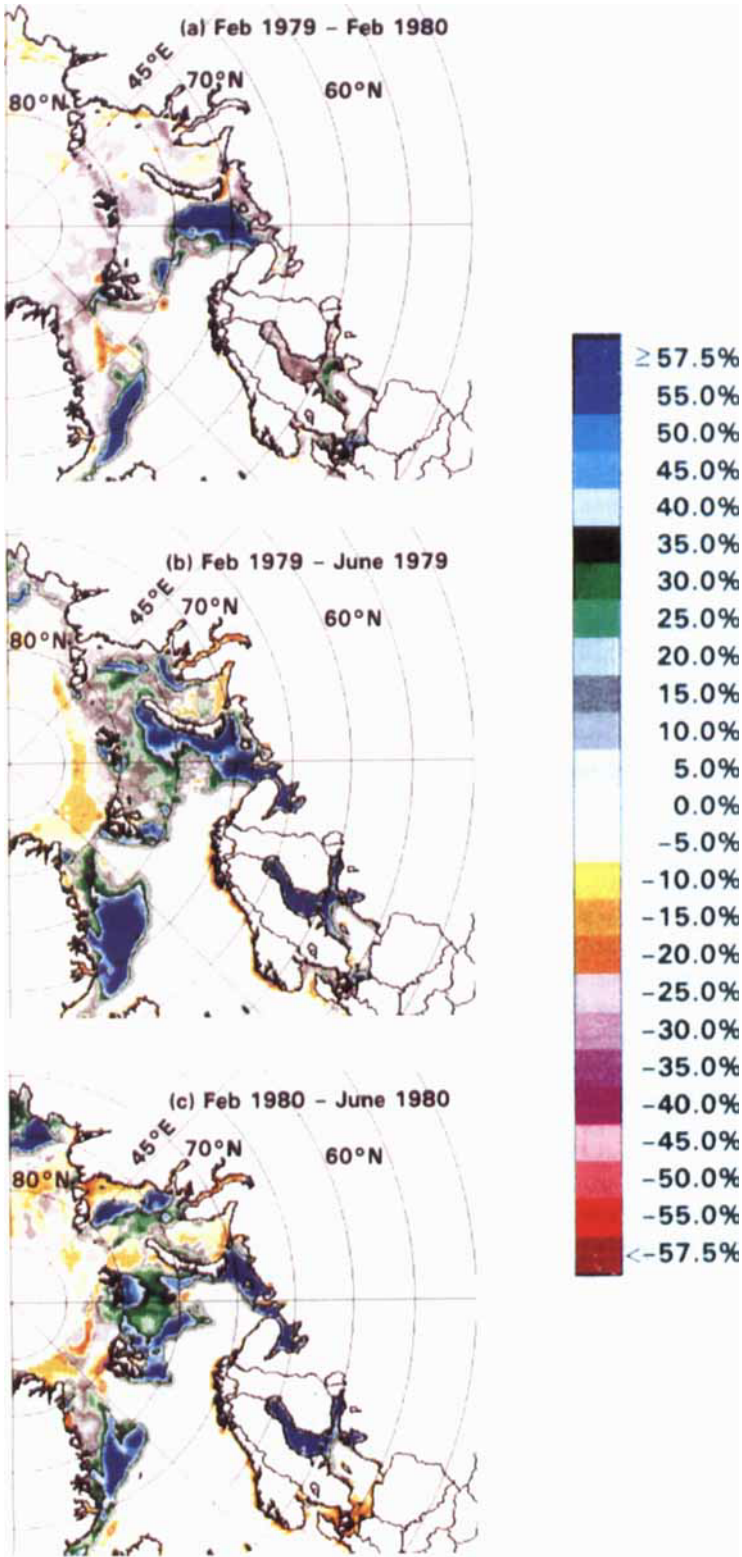


Fig. 10. Difference images of SMMR-derived sea ice concentrations: (a) February 1979–February 1980, (b) February 1979–June 1979, (c) February 1980–June 1980. Positive values (blue) correspond to less ice in the second image as compared to the first for the image pair that was differenced.

of fresh water advected into the Barents Sea from the Polar Basin and Kara Sea is unknown.

Satellite images of the sea ice dynamics and distributions of phytoplankton in 1979 and 1980 suggest a strong link between meteorological conditions (air temperature and sea ice extent) and the temporal structure of the ecosystems of the Barents Sea and adjacent waters. The extensive development of sea ice in 1979, and the large spring-summer recession, would have resulted in stronger, more southerly and earlier meltwater induced stratification in 1979 and compared to 1980. By contrast, minimal sea ice development in 1980 would result in minimal early stratification of the North Atlantic waters in the Barents Sea and adjacent regions.

We concur with the hypothesis of Skjoldal et al. (1987) that early and strong stratification in 1979 resulted in an early bloom in the Barents, Greenland and Norwegian Seas. By early July, according to this scenario, the surface nutrients were nearly depleted (Fig. 8A) resulting in minimal surface pigments (Figs. 7(a) and 8B). The lack of meltwater induced stratification in 1980, deduced from the sea ice maps and analysis of melt-water volumes, would not have promoted an early bloom with surface nutrient depletion. Again we concur with the hypothesis of Skjoldal et al. (1987) that the blooms observed in 1980 (Figs. 7(b) and 8D) resulted from summertime solar induced temperature stratification. We are indeed fortunate that the clear satellite imagery in 1979 and 1980 corresponded almost precisely to the timing of ship observations. However, the lack of a time-series of either CZCS or in situ observations precludes a rigorous evaluation of the hypotheses presented here or in Skjoldal et al. (1987). Clearly, future satellite missions must emphasize higher frequency coverage (as is already achieved for the sea ice observations) so that coupling of the ecological response to the physical forcing can be deduced with stronger statistical inference. This higher frequency coverage can be expected from the SeaWiFS mission to be launched by the United States National Aeronautics and Space Administration (NASA) in 1993 (Mitchell et al. 1991), and the Earth Observing System (EOS) scheduled for launch in the late 1990s. Complimentary environmental satellite missions by Japan, the European Community and other nations will supplement the data ensuring more complete information for seasonal, interannual and climatological scales.

A conceptual model of the Barents Sea ecosystem structure

The Barents Sea is a productive high-latitude sea which experiences large blooms upon the onset of spring stratification. Persistent and shallow summer stratification results in nutrient depletion of the surface waters. The spring bloom can support a large secondary production (Skjoldal et al. 1989; Loeng 1989a). Also, the region has been demonstrated to have massive events of organic matter sedimentation at the end of the spring bloom (Wassmann et al. 1990). Sedimenting organic matter can support the benthic community and may also be a means for net export of carbon from the atmosphere.

The low summertime surface phytoplankton concentrations in the central Barents Sea belie the massive subsurface blooms of phytoplankton that can only (and have been) observed by ship observations. The presence of these subsurface features is highly predictable during the summer; they persist and deepen as the season progresses from spring to autumn, eventually breaking down when overturning occurs in autumn. Although the 7-year mean CZCS imagery gives a false impression that the ecosystem is relatively unproductive, the ecosystem's predictability allows a more rational interpretation of the imagery. Satellite observations of sea ice, surface temperature and ocean color data may be capable of defining the timing and type (salinity, temperature) of spring stratification leading to a bloom. The ensuing surface bloom is easily quantified with ocean color imagery. The conceptual model presented here and more quantitatively in Støle-Hansen & Slagstad (1991) implies that the summertime condition is one of strong stratification, low surface nutrients and pigments, regardless of the mechanism of initial stratification. Such an understanding provides a framework for interpretation of post-bloom imagery. Satellites can be used to establish the timing, cause, duration and extent of the surface bloom; they are not as useful for directly estimating the production of an ecosystem such as the Barents Sea where most of the summer time new production occurs below the depth of observation of the satellite. Nevertheless, coupled with the ecosystem's summer time predictability, the satellite observations can provide data that would be useful for forcing an ecosystem model that is capable of being updated by satellite observations.

Conclusions

A cursory evaluation of the 7-year mean CZCS imagery of the productive Barents Sea indicates that it is an oligotrophic or mesotrophic body of water. The imagery does reveal a distinctive meridional zonation of the ecosystem structure with apparently higher phytoplankton crops in the coastal and Atlantic waters. That structure is well-correlated with the complex hydrographic circulation of the region. For ocean color data to be most useful for practical applications, higher frequency coverage is essential and detailed regional bio-optical relationships should be defined (e.g. Mitchell & Holm-Hansen 1991a; Mitchell 1991). The next generation of sensors, including SeaWiFS, the EOS-era sensors and the Japanese and European Community systems will provide the essential high frequency coverage. Fisheries management should embrace the new technology and ensure that the local high-resolution data are collected so that they may be evaluated for their utility in commercial applications. Studies of the regional bio-optical relationships should be part of a comprehensive monitoring plan.

This case study is an example of the need to use multi-platform observations (ship and satellite in this case) and multisensor (SMMR, CZCS) satellite data, to make deductions on the functional aspects of a complicated and dynamic ecosystem. Clearly, satellites alone cannot provide the detailed knowledge of ocean ecosystems required for a thorough understanding. However, together with ship observations, satellites provide the ability for greater temporal and spatial sampling required for hypothesis testing. The combined approach must be focused on developing regional models of ecosystem function which can then be linked to create basin-scale models.

Fisheries management of the Barents Sea system may benefit greatly from utilization of satellite remote sensing data. Satellites can easily define the ice boundaries and kinematics as well as winds, sea surface temperature and surface phytoplankton concentrations. These data could be used as input to detailed ecosystems models that are forced by meteorological factors, water mass distributions and ice conditions. Much evidence collected in the Barents Sea, including the detailed studies of the Pro Mare program in the 1980s, has demonstrated that interannual variability in the year-class recruitment of com-

mercially important species, and their planktonic food, are coupled to the physical structure of the Barents Sea ecosystem (Skjoldal et al. 1987; Skjoldal & Rey 1989; Loeng 1989a; Loeng 1989b). Description of that structure in a timely fashion to be effectively used for fisheries management policy decisions is not possible using ship-based observations alone.

Acknowledgements. – We thank the members of the Pro Mare program, in particular the Chairman, E. Sakshaug, for their gracious invitation to participate in Pro Mare Cruise 11. The efforts of the Captain and Crew of R/V G. O. SARS during that cruise are gratefully acknowledged. We also thank F. Rey and H. Loeng for nutrient, chlorophyll, salinity and temperature data from Pro Mare Cruise 11 and from their work in 1979 and 1980; V. Spode for analysis and graphics; M. Vernet, H. Sosik and two anonymous reviewers for critical reviews of a draft of the manuscript. This work was supported by grants from the National Science Foundation (DPP-8520848), the National Aeronautics and Space Administration (NAGW-1070; and RTPO #'s 579-11-01-20; 579-11-03-20; 461-62-09-01) and the Office of Naval Research (N00014-89-J-1639).

References

- Ådlandsvik, B. & Loeng, H. 1991: A study of the climatic system in the Barents Sea. Pp. 45–49 in Sakshaug, E., Hopkins, C. C. E. & Øritsland, N. A. (eds.): Proceedings of the Pro Mare Symposium on Polar Marine Ecology. Trondheim, 12–16 May 1990. *Polar Research 10(1)*.
- Bartz, R., Zaneveld, J. R. V. & Pak, H. 1978: A transmissometer for profiling and moored observations in water. Pp. 102–108 in White, M. B. & Stevenson, R. E. (eds.): *Ocean Optics V. SPIE*, Bellingham, Washington.
- Cosmiso, J. C. 1986: Characteristics of winter sea ice from satellite multispectral microwave observations. *J. Geophys. Res.* 91, 975–994.
- Feldman, G., Kuring, N., Ng, C., Esaias, W., McClain, C., Elrod, J., Maynard, N. G., Endres, N., Evans, R., Brown, J., Walsh, J., Carl, M. & Podesta, G. 1989: Ocean Color: Availability of the global data set. *Eos 70(23)*, 634–643.
- Gordon, H. R., Clark, D. K., Brown, J. W., Brown, O. B., Evans, R. H. & Broenkow, W. W. 1983: Phytoplankton pigment concentrations in the Middle Atlantic Bight: comparison of ship determinations and CZCS estimates. *Appl. Optics 22*, 20–36.
- Gordon, H. R., Clark, D. K., Mueller, J. L. & Hovis, W. A. 1980: Phytoplankton pigments from the Nimbus-7 Coastal Zone Color Scanner: Comparison with surface measurements. *Science 210*, 63–66.
- Gordon, H. R. & McCluney, R. W. 1975: Estimation of the depth of sunlight penetration in the sea for remote sensing. *Appl. Optics 14*, 413–416.
- Holm-Hansen, O., Lorenzen, C. J., Holmes, R. W. & Strickland, J. D. H. 1965: Fluorimetric determination of chlorophyll. *J. Cons. Perm. Int. Explor. Mer 30*, 3–15.
- Loeng, H. 1989a: Ecological features of the Barents Sea. In Rey, L. & Alexander, V. (eds.): *Proc. 6th Conf. Comité Arctique Internat.*, 13–15 May 1985. E. J. Brill, New York.

- Loeng, H. 1989b: The influence of temperature on some fish population parameters in the Barents Sea. *J. Northw. Atl. Fish. Sci.* 9, 103–113.
- Loeng, H. 1991: Features of the physical oceanographic conditions of the Barents Sea. Pp. 5–18 in Sakshaug, E., Hopkins, C. C. E. & Øritsland, N. A. (eds.): Proceedings of the Pro Mare Symposium on Polar Marine Ecology, Trondheim, 12–16 May 1990. *Polar Research* 10(1).
- McClain, C. R., Darzi, M., Firestone, J. K., Fu, G., Yeh, E.-N. & Endres, D. L. 1991: *SEAPAK User's Guide, Version 2, Tech. Memo 100728*. NASA/GSFC, Greenbelt, MD.
- Mitchell, B. G. 1991: Predictive bio-optical relationships for polar oceans and marginal ice zones. *J. Mar. Syst.* 3(1/2), 91–105.
- Mitchell, B. G. & Holm-Hansen, O. 1991a: Bio-optical properties of Antarctic waters: Differentiation from temperate ocean models. *Deep Sea Res.* 38(8/9), 1009–1028.
- Mitchell, B. G. & Holm-Hansen, O. 1991b: Observations and modeling of the Antarctic phytoplankton crop in relation to mixing depth. *Deep Sea Res.* 38(8/9), 981–1007.
- Mitchell, B. G., Esaias, W. E., Feldman, G. C., Kirk, R. G., McClain, C. R. & Lewis, M. R. 1991: Satellite ocean color data for studying oceanic biogeochemical cycles. *Proceedings IEEE*, 283–287.
- Mueller, J. L. 1988: Nimbus-7 CZCS: electronic overshoot due to cloud reflectance. *Appl. Optics* 27(3), 438–440.
- Rey, F. & Loeng, H. 1985: The influence of ice and hydrographic conditions on the development of phytoplankton in the Barents Sea. Pp. 49–63 in Gray, J. S. & Christiansen, M. E. (eds.): *Marine biology of polar regions and effects of stress in marine organisms*. John Wiley and Sons Ltd., New York.
- Rey, F., Skjoldal, H. R. & Slagstad, D. 1987: Primary production in relation to climatic changes in the Barents Sea. Pp. 29–46 in Loeng, H. (ed.): *The effect of oceanographic conditions on distribution and population dynamics of commercial fish stocks in the Barents Sea*. Proc. the 3rd Soviet–Norwegian Symposium, Murmansk, 26–28 May 1986.
- Skjoldal, H. R., Hassel, A., Rey, F. & Loeng, H. 1987: Spring phytoplankton development and zooplankton reproduction in the Barents Sea in the period 1979–1984. Pp. 59–89 in Loeng, H. (ed.): *The effect of oceanographic conditions on distribution and population dynamics of commercial fish stocks in the Barents Sea*. Proc. 3rd Soviet–Norwegian Symposium, Murmansk, 26–28 May 1986. Inst. Mar. Res., Bergen.
- Skjoldal, H. R. & Rey, F. 1989: Pelagic production and variability of the Barents Sea ecosystem. Pp. 241–286 in Sherman, K. & Alexander, L. M. (eds.): *Biomass Yields and Geography of Large Marine Ecosystems*. American Association for the Advancement of Science, New York.
- Støle-Hansen, K. & Slagstad, D. 1991: Simulation of currents, ice-melting, and vertical mixing in the Barents Sea using a 3-D baroclinic model. Pp. 33–44 in Sakshaug, E., Hopkins, C. C. E. & Øritsland, N. A. (eds.): Proceedings of the Pro Mare Symposium on Polar Marine Ecology, Trondheim, 12–16 May 1990. *Polar Research* 10(1).
- Strickland, J. D. H. & Parsons, T. R. 1972: A practical handbook of seawater analysis. *Bull. Fish. Res. Board Can.* 167, 1–311.
- Sverdrup, H. U. 1953: On conditions for the vernal blooming of phytoplankton. *J. Cons. Perm. Int. Explor. Mer* 18, 287–295.
- Wassmann, P., Vernet, M., Mitchell, B. G. & Rey, F. 1990: Mass sedimentation of *Phaeocystis pouchetii* in the Barents Sea. *Mar. Ecol. Prog. Ser.* 66, 183–195.